Specific heat of MgB_2 in a one- and a two-band model from first-principles calculations

2002 J. Phys.: Condens. Matter 14 1353

(http://iopscience.iop.org/0953-8984/14/6/320)

INSTITUTE OF PHYSICS PUBLISHING JOURNAL OF PHYSICS: CONDENSED MATTER

J. Phys.: Condens. Matter **14** (2002) 1353–1360 PII: S0953-8984(02)31185-8

Specific heat of MgB_2 in a one- and a two-band model from first-principles calculations

A A Golubov[1], J Kortus[2], O V Dolgov[2], O Jepsen[2], Y Kong[2], O K Andersen[2], B J Gibson[2], K Ahn[2] and R K Kremer[2]

[1] University of Twente, Department of Applied Physics, 7500 AE Enschede, The Netherlands
[2] Max-Planck-Institut für Festkörperforschung, Heisenbergstrasse 1, D-70569 Stuttgart, Germany

E-mail: j.kortus@fkf.mpg.de

Received 23 November 2001, in final form 10 January 2002
Published 1 February 2002
Online at stacks.iop.org/JPhysCM/14/1353

Abstract

The heat capacity anomaly at the transition to superconductivity of the layered superconductor MgB_2 is compared to first-principles calculations with the Coulomb repulsion, μ^*, as the only parameter which is fixed to give the measured T_c. We solve the Eliashberg equations for both an isotropic one-band model and a two-band model with different superconducting gaps on the π-band and σ-band Fermi surfaces. The agreement with experiments is considerably better for the two-band model than for the one-band model.

(Some figures in this article are in colour only in the electronic version)

1. Introduction

The nature of the superconducting state in MgB_2 has been characterized by a broad range of experimental and theoretical methods, and many basic properties have been unambiguously established since the discovery of the 40 K superconductor MgB_2 by Nagamatsu and collaborators [1].

While electron–phonon coupling as the underlying pairing mechanism has been pinpointed by a large B isotope effect on T_c, proving B-related vibrations to be essential [2, 3], the nature of the order parameter (namely the superconducting gap) has remained a matter of debate. The order parameter has been intensively investigated by tunnelling and point contact spectroscopy [4–16] as well as by high-resolution photoelectron spectroscopy [17,18]. While these techniques show an energy gap in the quasiparticle spectrum most probably of s-wave symmetry, the magnitude of the gap, $\Delta(0)$, itself remained an open question: tunnelling experiments initially revealed a distribution of energy gaps with lower boundary $2\Delta_1(0)/k_BT_c \approx 1.1$ and upper boundary $2\Delta_2(0)/k_BT_c \approx 4.5$. These values are either considerably lower or distinctly larger than the weak-coupling BCS value of $2\Delta(0)/k_BT_c = 3.53$, and these controversial findings have been discussed in terms of gap anisotropy

or more recently attributed to the presence of two gaps or multiple gaps [12, 18]. The analysis of the electronic Raman continuum of MgB_2 by Chen *et al* [13] also pointed to the presence of two gaps with gap values within the limits indicated by the tunnelling experiments [19].

While these experiments employ surface-sensitive techniques to determine the gap properties, evidence for multigap behaviour emerges also from methods like heat capacity or μSR measurements probing true bulk properties[3]. In the early heat capacity experiments a typical jump-like anomaly is seen at T_c whose magnitude $\Delta C_p/T_c$ amounts at best to only about 70–80% of the value $1.43\gamma^N(T_c)$ predicted by weak-coupling BCS theory [2, 21–25]. $\gamma^N(T_c)$ is the Sommerfeld constant in the normal state which was obtained from heat capacity measurements in high magnetic fields and which was determined to be 2.7–3 mJ mol^{-1} K^{-2}. The shape of the heat capacity anomaly compares reasonably well with BCS-type behaviour assuming $2\Delta(0)/k_BT_c = 3.53$ with appropriately adjusted magnitude. An improved fit of the detailed temperature dependence of the heat capacity anomaly was obtained when calculating the heat capacity within the α-model [26] assuming a BCS temperature dependence of the gap but with an increased ratio $2\Delta(0)/k_BT_c = 4.2(2)$ [21]. This result matches very well with the upper limit of the gap value consistently found in the tunnelling experiments and was suggested as evidence that MgB_2 is in the moderately strong-coupling limit. More recently, the excess heat capacity observed close to $T_c/4$ by Bouquet *et al* [22] and Wang *et al* [24] has been attributed to a second smaller gap. Fits with a phenomenological two-gap model assuming that the heat capacity of MgB_2 can be decomposed as a sum of the two individual heat capacities gave a very good description with gap values of $2\Delta_1(0)/k_BT_c = 1.2(1)$ and $2\Delta_2(0)/k_BT_c \approx 4$ [27]. Recent muon-spin-relaxation measurements of the magnetic penetration depth are consistent with a two-gap model [28].

Theoretically, multigap superconductivity in MgB_2 was first proposed by Shulga *et al* [29] to explain the behaviour of the upper critical magnetic field. On the basis of the electronic structure, the existence of multiple gaps has been suggested by Liu *et al* [30] in order to explain the magnitude of T_c. The electronic structure of MgB_2 contains four Fermi surface sheets [31]. Two of them with 2D character emerging from bonding σ-bands form small cylindrical Fermi surfaces around Γ–A. The other two originating from bonding and antibonding π-bands have 3D character and form a tubular network. Liu *et al* [30] conclude from first-principles calculations of the electron–phonon coupling that the superconducting gaps are different for the individual sheets and they obtain two different order parameters, a larger one on the 2D Fermi surface sheets and a second gap on the 3D Fermi surfaces; the latter was estimated to be approximately a factor of three less than the former.

In the present paper we calculate the specific heat capacity from the spectral Eliashberg function $\alpha^2(\omega)F(\omega)$ first in the one-band model using the isotropic $\alpha^2(\omega)F(\omega)$ function as given by Kong *et al* [32]. Then we calculate the heat capacity in a two-band model by reducing the sixteen Eliashberg functions $\alpha^2_{ij}(\omega)F_{ij}(\omega)$ appropriate for the four Fermi surface sheets to four Eliashberg functions corresponding to an effective-two-band model with a σ-band and π-band only. From the solution of the Eliashberg equations we obtain a superconducting gap ratio $\Delta_\sigma/\Delta_\pi \simeq 2.63$ in good agreement with the experimental data. The two-band model explains the reduced magnitude of the heat capacity anomaly at T_c very well and also reproduces the experimental observed excess heat capacity at low temperatures.

[3] Heat capacity experiments are a classical tool for identifying multiple gaps in superconductors. For example, strong evidence for two energy gaps has been gained from heat capacity measurements on high-purity crystals of the elemental superconductors Nb, Ta, and V (cf [20]).

2. Theory

2.1. One-band model

First we discuss the specific heat in the isotropic single-band model with a strong (intermediate) electron–phonon interaction (EPI). In the normal state and in the adiabatic approximation the electronic contribution to the specific heat is determined from the Eliashberg function $\alpha^2(\omega)F(\omega)$ by means of the expression [33]

$$C_N^{el}(T) = (2/3)\pi^2 N(0) k_B^2 T \left[1 + (6/\pi k_B T) \int_0^\infty f(\omega/2\pi k_B T)\alpha^2(\omega)F(\omega)\,\mathrm{d}\omega \right] \tag{1}$$

where $N(0)$ is a bare density of states per spin at the Fermi energy. The kernel $f(x)$ is expressed in terms of the derivatives of the digamma function $\psi(x)$:

$$f(x) = -x - 2x^2\,\mathrm{Im}\,\psi'(\mathrm{i}x) - x^3\,\mathrm{Re}\,\psi''(\mathrm{i}x). \tag{2}$$

At low temperatures the specific heat has the well known asymptotic form $C_N^{el}(T \to 0) = (1+\lambda)\gamma_0 T$, where $\lambda = 2\int_0^\infty \mathrm{d}\omega\,\omega^{-1}\alpha^2(\omega)F(\omega)$ is the electron–phonon coupling constant and $\gamma_0 = 2\pi^2 k_B^2 N(0)/3$ is the specific heat coefficient for non-interacting electrons. At higher temperatures the specific heat differs from this trivial expression (see the discussion in [34]).

For the superconducting state, an expression for the specific heat obtained by Bardeen and Stephen [35] which is based on an *approximate* sum rule has often been used. We shall however use an *exact* expression for the thermodynamical potential in the electron–phonon system which is based on the integration of the electronic Green function over the coupling constant:

$$\Omega = \Omega_{el}^{(0)} + \Omega_{ph}^{(0)} + T\sum_{\omega_n} \int_0^1 \frac{\mathrm{d}x}{x}\,\mathrm{tr}[\hat{\Sigma}(x)\hat{G}(x)] \tag{3}$$

where x is dimensionless; $\hat{G}(x)$ and $\hat{\Sigma}(x)$ are the exact electron Green function and the self-energy, respectively, for a coupling constant of $x\lambda$. The functions $\Omega_{el}^{(0)}$ and $\Omega_{ph}^{(0)}$ are the thermodynamic potentials for non-interacting electrons and non-interacting phonons, respectively. Some further arithmetic leads to the expression for the difference between the free energies, F_N and F_S, of the superconducting and normal state [36]:

$$-\frac{F_N - F_S}{\pi N(0) T} = \sum_{n=-\omega_c}^{\omega_c} \left\{ |\omega_n|(Z^N(\omega_n) - 1) - \frac{2\omega_n^2[(Z^S(\omega_n))^2 - 1] + \varphi_n^2}{|\omega_n| + \sqrt{\omega_n^2(Z^S(\omega_n))^2 + \varphi_n^2}} + \frac{\omega_n^2 Z^S(\omega_n)(Z^S(\omega_n) - 1) + \varphi_n^2}{\sqrt{\omega_n^2(Z^S(\omega_n))^2 + \varphi_n^2}} \right\} \tag{4}$$

where $Z(\omega_n)$ is a normalization factor, $\varphi_n = \Delta_n/Z(\omega_n)$ is an order parameter and Δ_n is the gap function.

The specific heat at temperature T is calculated according to

$$\Delta C_{el}(T) = T\,\partial^2(F_N - F_S)/\partial T^2. \tag{5}$$

The specific heat jump $\Delta C_{el}(T_c)$ at $T = T_c$ is determined by the coefficient $\beta = T_c\,\Delta C_{el}(T_c)/2$ in $F_N - F_S = \beta t^2$, where $t = (T_c - T)/T_c$.

2.2. Two-band model

We have calculated the sixteen Eliashberg functions $\alpha_{ij}^2(\omega)F_{ij}(\omega)$ where i and j label the four Fermi surface sheets and thereafter combined them into four corresponding to an *effective*-two-band model which contains only a σ- and a π-band. Their respective

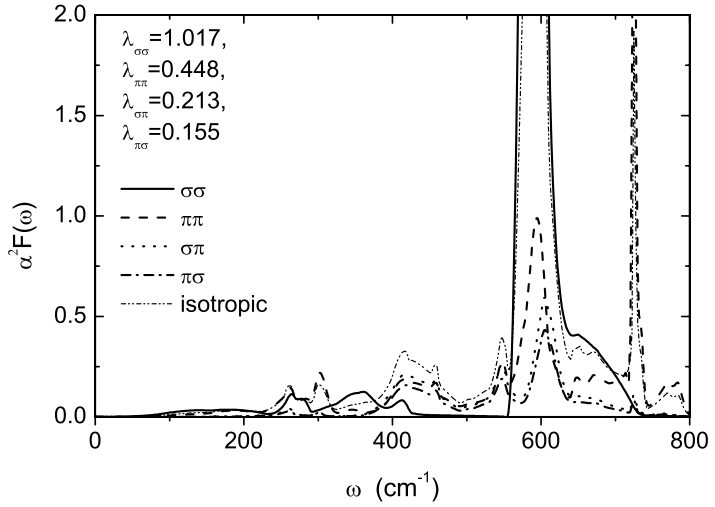

Figure 1. The four superconducting Eliashberg functions $\alpha^2 F(\omega)$ obtained from first-principles calculations for the effective-two-band model and the isotropic Eliashberg function for the one-band model. The coupling constant of the isotropic one-band model has a value of $\lambda_{iso} = 0.87$.

densities of states at the Fermi energy have values of $N_\sigma(0) = 0.300$ states eV^{-1}/cell and $N_\pi(0) = 0.410$ states eV^{-1}/cell. Similar coupling constants $\lambda_{\sigma\sigma}$, $\lambda_{\pi\pi}$, $\lambda_{\sigma\pi}$, and $\lambda_{\pi\sigma}$ which are required for a two-band model were calculated earlier in [30]. The procedure of reducing the sixteen Eliashberg functions of the real four-band system due to the four different Fermi surface sheets to an effective-two-band model with only four coupling constants λ_{ij} is an approximation which is based on the similarity of the two cylindrical and the two three-dimensional sheets of the Fermi surface, requiring the same physical properties in both σ-bands or both π-bands. More details can be found elsewhere [37].

The four Eliashberg functions $\alpha^2_{ij}(\omega)F_{ij}(\omega)$ for the effective-two-band model are shown in figure 1. The most significant contribution comes from the coupling of the bond-stretching phonon modes to the σ-band. The coupling constants corresponding to the superconducting Eliashberg functions have been calculated to be $\lambda_{\sigma\sigma} = 1.017$, $\lambda_{\pi\pi} = 0.448$, $\lambda_{\sigma\pi} = 0.213$, and $\lambda_{\pi\sigma} = 0.155$. The small difference from the values given in [30] may be attributed to the different first-principles methods used in the calculations of the Eliashberg functions.

Besides the spectral functions we need to know the Coulomb matrix element μ_{ij}. With the help of the wavefunctions from our first-principles calculations we can approximately calculate the ratios for the μ-matrix [37]. The $\sigma\sigma$-, $\pi\pi$-, and $\sigma\pi$-values were in the ratio 2.23/2.48/1. This allows one to express $\mu^*_{ij}(\omega_c)$ in terms of these ratios and one single free parameter, which is fixed, to get the experimental T_c of 39.4 K from the solution of the Eliashberg equations. The $\mu^*(\omega_c)$ matrix elements determined by this procedure are $\mu^*_{\sigma\sigma}(\omega_c) = 0.210$, $\mu^*_{\sigma\pi}(\omega_c) = 0.095$, $\mu^*_{\pi\sigma}(\omega_c) = 0.069$, and $\mu^*_{\pi\pi}(\omega_c) = 0.172$.

Using our calculated Eliashberg functions on the imaginary (Matsubara) axis together with the above matrix $\mu^*_{ij}(\omega_c)$, we obtain the gap values $\Delta_\sigma = \lim_{T\to 0} \Delta_\sigma(\mathrm{i}\pi T) \simeq 7.1$ meV, and $\Delta_\pi \simeq 2.7$ meV, which corresponds to $2\Delta_\sigma/k_BT_c = 4.18$ and $2\Delta_\pi/k_BT_c = 1.59$. The temperature dependences of the superconducting gaps are shown in figure 2. The filled circles (squares) display the gap for the 2D σ-band (3D π-band). Due to interband coupling between the bands, both gaps close, at the same critical temperature. For comparison, the BCS curve (line) is also shown for a single gap (one-band-model) which closes at $T_c = 39.4$ K. The corresponding single BCS gap would be 6 meV.

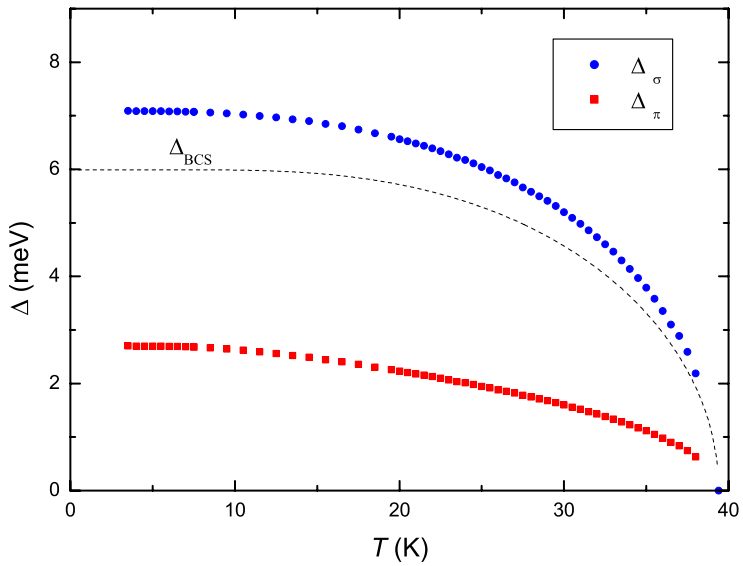

Figure 2. The temperature dependences of the superconducting gaps from the solution of the two-band Eliashberg equations. The values of the gaps at $T = 0$ K were obtained as $\Delta_\sigma(T = 0) = 7.1$ meV and $\Delta_\pi(T = 0) = 2.7$ meV. The BCS value for the gap that corresponds to $T_c = 39.4$ K is 6.0 meV at 0 K.

The extension of equation (1) to the two-band model gives

$$C_{el}^N(T) = \frac{2\pi^2}{3} N_{tot}(0) k_B^2 T + 4\pi k_B [N_\sigma(0)(I_{\sigma\sigma} + I_{\sigma\pi}) + N_\pi(0)(I_{\pi\pi} + I_{\pi\sigma})] \tag{6}$$

where $I_{ij} = \int_0^\infty f(\omega/2\pi k_B T)\alpha_{ij}^2(\omega)F_{ij}(\omega)\,\mathrm{d}\omega$ $(i, j = \pi, \sigma)$, and the function $f(x)$ is given by equation (2).

The generalization of the superconducting free energy (4) to the two-band model is straightforward, and the heat capacity was obtained according to equation (5).

3. Comparison with experiment

For the comparison with experiment we have selected data obtained by our group [21] and by Bouquet *et al* [22]. The anomaly clearly visible at T_c in the zero-field data is suppressed by a magnetic field of 9 T in both experiments. In figure 3 we display the difference $\Delta C_p = C_p(0\ \mathrm{T}) - C_p(9\ \mathrm{T})$. The anomalies at T_c detected by the two groups clearly have different magnitudes: the one described in [22] amounts to 133 mJ mol^{-1} K^{-1} at T_c and represents the largest specific heat capacity anomaly reported for MgB_2 so far[4]; the $\Delta C_p(T_c)$ reported by our group is somewhat smaller. However, the shapes of the anomalies close to T_c are very similar for the two samples. In fact, fitting the anomalies with the α-model revealed identical ratios: $2\Delta/k_B T_c = 4.2$ with $\Delta = 7$ meV for both samples [21, 22, 27].

First we will try to discuss the experimental results in terms of a conventional one-band model. The specific heat in MgB_2 was calculated using the isotropic spectral Eliashberg function $\alpha^2(\omega)F(\omega)$ of Kong *et al* [32]. This function yields an electron–phonon coupling

[4] It is interesting that experiments on different samples show similar values for the specific heat jump $\Delta C \simeq 113$ mJ mol^{-1} K^{-1} [2], $\Delta C \simeq 81$ mJ mol^{-1} K^{-1} [24], $\Delta C \simeq 133$ mJ mol^{-1} K^{-1} [22], $\Delta C \simeq 125$ mJ mol^{-1} K^{-1} [23], $\Delta C \simeq 115$ mJ mol^{-1} K^{-1} [25], $\Delta C \simeq 92$ mJ mol^{-1} K^{-1} [38].

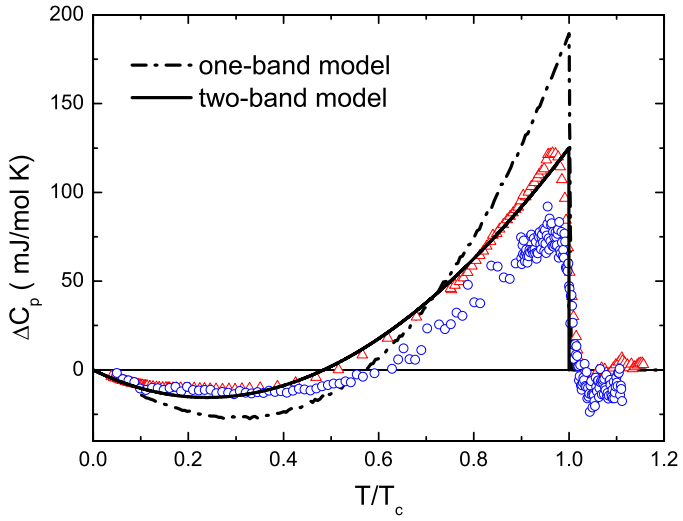

Figure 3. Experimental data on the heat capacity difference $\Delta C_p = C_p(0\,\mathrm{T}) - C_p(9\,\mathrm{T})$ from [21] (○) and from [22] (△). The dashed curve is the theoretical result from the one-band model and the thick solid curve corresponds to the two-band model, from the solution of the Eliashberg equations. The two-band model reproduces the specific heat jump as well as the low-temperature behaviour much better.

constant $\lambda = 0.87$ and, together with a Coulomb pseudopotential of $\mu^* = 0.1$, yields $T_c = 40$ K. The calculated specific heat at T_c is $\gamma^N(T_c) = 1.94\gamma_0 = 3.24$ mJ mol^{-1} K^{-2} with $\gamma_0 = 1.67$ mJ mol^{-1} K^{-2} from the band-structure calculations of [31, 32]. The specific heat jump at T_c equals $\Delta C \simeq 196$ mJ mol^{-1} K^{-1}, which is a factor of 1.5–2 larger than the experimental values (see footnote 4). This corresponds to $\Delta C/(\gamma^N(T_c)T_c) \simeq 1.51$, compared to the BCS value of 1.43. The difference $\Delta C_{el}(T) = C_{el}^S(T) - C_{el}^N(T)$ is shown in figure 3 (dash–dot curve) in comparison with the experimental data. Not only does the size of the jump disagree with the experiment, but also the behaviour at low temperatures is different. The latter is connected with the fact that at low temperature equation (4) for a single-band model leads to the standard exponential dependence $C^S \sim T^{-3/2}\exp(-\Delta/T)$, while the experimental data show a more complicated behaviour. Clearly there exists a discrepancy between experimental data and a theoretical one-band model.

The solid curve in figure 3 represents the theoretical results for the two-band model as described above. The low-temperature behaviour is in much better agreement with the experiment. The specific heat jump is now significantly reduced in comparison with a single-band model and reproduces surprisingly well the experimental data of [22]. With the data given above we obtain from our theoretical calculation an electronic heat capacity in the normal state of $\gamma^N(T_c) = C_{el}^N(T_c)/T_c \simeq 3.24$ mJ mol^{-1} K^{-2}, the same value as for the one-band model. The absolute value of the specific heat jump in the two-band model is $\Delta C \simeq 125$ mJ mol^{-1} K^{-1}, corresponding to $\Delta C/(\gamma^N(T_c)T_c) \simeq 0.98$ which is now smaller than the BCS value.

We would like to emphasize here that no fitting is involved in the theoretical calculations. The only free parameter, which is in the Coulomb matrix elements, is already determined by the experimental T_c of 39.4 K.

One could suspect that the difference between the theoretical results from the effective-two-band model and our experimental data may be attributable to a different amount of impurities in the samples compared to the samples of [22]. In the one-band model the critical

temperature T_c as well as the value and the temperature dependence of $\Delta C_p(T)$ are not affected by non-magnetic impurities (Anderson theorem). This is in complete contrast to the situation for the two-band model, where both quantities are strongly dependent on *interband* impurity scattering. Interband impurity scattering leads to averaging of the gaps and thus to increase of the $\Delta C_p/\gamma^N(T_c)T_c$ ratio. On the other hand, due to the decrease of T_c, the specific heat jump only depends weakly on the scattering strength. In order to investigate the dependence of T_c and of ΔC_p on the interband impurity scattering, we included the effect of interband impurities in the Eliashberg equations. The results show that even for rather strong impurity scattering $1/2\tau = 3\pi T_{c0} \simeq 371$ K, which leads to a drastic change of the critical temperature (decreasing to $T_c = 29.4$ K) and strong averaging of the gaps, the specific heat jump remains practically unchanged: $\Delta C_p \simeq 120$ mJ mol^{-1} K^{-1}. This corresponds to a ratio $\Delta C_p/\gamma(T_c)T_c \simeq 1.48$, which is very close to the corresponding value for a single-gap model. Therefore, interband impurity scattering can explain the change of T_c in different samples, but is not responsible for the observed different values of the specific heat capacity anomaly at T_c.

We have shown that a complete theoretical calculation from first principles using an effective-two-band model can explain the major features in the specific heat measurement of MgB_2 surprisingly well. The theoretical framework presented goes beyond a simple phenomenological two-gap model, because interband effects are included explicitly and no fitting to experimental results has been performed. The reduced value of the heat capacity anomaly at T_c as well as the low-temperature behaviour are in excellent agreement with experimental results. The same first-principles approach using exactly the same Eliashberg functions and Coulomb matrix elements has been used in order to explain optical measurements [37] and tunnelling experiments [39] on the interesting superconductor MgB_2.

Acknowledgment

JK would like to thank the Schloeßmann Foundation for financial support.

References

[1] Akimitsu J 2001 *Symp. on Transition Metal Oxides (Sendai, Jan. 2001)*
Nagamatsu J, Nakagawa N, Muranaka T, Zenitani Y and Akimitsu J 2001 *Nature* **410** 63
[2] Bud'ko S L, Lapertot G, Petrovic C, Cunningham C E, Anderson N and Canfield P C 2001 *Phys. Rev. Lett.* **86** 1877
[3] Hinks D G, Claus H and Jorgensen J D 2001 *Nature* **411** 457
[4] Karapetrov G, Iavarone M, Kwok W K, Crabtree G W and Hinks D G 2001 *Phys. Rev. Lett.* **86** 4374
[5] Schmidt H, Zasadzinski J F, Gray K E and Hinks D G 2001 *Phys. Rev.* B **63** 220504(R)
[6] Rubio-Bollinger G, Suderow H and Vieira S 2001 *Phys. Rev. Lett.* **86** 5582
[7] Sharoni A, Felner I and Millo O 2001 *Phys. Rev.* B **63** 220508
[8] Kohen A and Deutscher G 2001 *Phys. Rev.* B **64** 060506(R)
[9] Plecenik A, Beňačka Š, Kúš P and Grajcar M 2001 *Preprint* cond-mat/0104038
[10] Szabó P, Samuely P, Kacmarcik J, Klein T, Marcus J, Fruchart D, Miraglia S, Marcenat C and Jansen A G M 2001 *Phys. Rev. Lett.* **87** 137005
[11] Giubileo F, Roditchev D, Sacks W, Lamy R and Klein J 2001 *Preprint* cond-mat/0105146
[12] Giubileo F, Roditchev D, Sacks W, Lamy R, Thanh D X, Klein J, Miraglia S, Fruchart D, Marcus J and Monod P 2001 *Phys. Rev. Lett.* **87** 177008
[13] Chen C-T, Seneor P, Yeh N-C, Vasquez R P, Jung C U, Park M-S, Kim H-J, Kang W N and Lee S-I 2001 *Preprint* cond-mat/0104285
[14] Laube F, Goll G, Hagel J, von Löhneysen H, Ernst D and Wolf T 2001 *Europhys. Lett.* **56** 296–301
[15] Zhang Y, Kinion D, Chen J, Hinks D G, Crabtree G W and Clarke J 2001 *Preprint* cond-mat/0107478
[16] Bugoslavsky Y, Miyoshi Y, Perkins G K, Berenov A V, Lockman Z, MacManus-Driscoll J L, Cohen L F and Caplin A D 2001 *Preprint* cond-mat/0110296

[17] Takahashi T, Sato T, Souma S, Muranaka T and Akimitsu J 2001 *Phys. Rev. Lett.* **86** 4915
[18] Tsuda S, Yokoya T, Kiss T, Takano Y, Togano K, Kitou H, Ihara H and Shin S 2001 *Phys. Rev. Lett.* **87** 177006
[19] Chen X K, Konstantinovič M J, Irwin J C, Lawrie D D and Franck J P 2001 *Phys. Rev. Lett.* **87** 157002
[20] Meservey R and Schwartz B B 1969 *Superconductivity* ed R D Parks (New York: Dekker) and references to the original work therein
[21] Kremer R K, Gibson B J and Ahn K 2001 *Preprint* cond-mat/0102432
[22] Bouquet F, Fisher R A, Phillips N E, Hinks D G and Jorgensen J D 2001 *Phys. Rev. Lett.* **87** 047001
[23] Wälti C, Felder E, Degen C, Wigger G, Monnier R, Delley B and Ott H R 2001 *Phys. Rev.* B **64** 172515
[24] Wang Y, Plackowski T and Junod A 2001 *Physica* C **355** 179
[25] Yang H D, Lin J-Y, Li H H, Hsu F H, Liu C J and Jin C 2001 *Phys. Rev. Lett.* **87** 167003
[26] Padamsee H, Neighbor J E and Shifman C A 1973 *J. Low Temp. Phys.* **12** 387
[27] Bouquet F, Wang Y, Fisher R A, Hinks D G, Jorgensen J D, Junod A and Phillips N E 2001 *Europhys. Lett.* **56** 856
[28] Niedermayer C, Bernhard C, Holden T, Kremer R K and Ahn K 2001 *Preprint* cond-mat/018431
[29] Shulga S V, Drechsler S-L, Eschrig H, Rosner H and Pickett W E 2001 *Preprint* cond-mat/0103154
[30] Liu A Y, Mazin I I and Kortus J 2001 *Phys. Rev. Lett.* **87** 087008
[31] Kortus J, Mazin I I, Belashchenko K D, Antropov V P and Boyer L L 2001 *Phys. Rev. Lett.* **86** 4656
[32] Kong Y, Dolgov O V, Jepsen O and Andersen O K 2001 *Phys. Rev.* B **64** 020501(R)
[33] Grimvall G 1981 *Electron–Phonon Interaction in Metals* (Amsterdam: North-Holland)
[34] Shulga S V, Dolgov O V and Mazin I I 1992 *Physica* C **192** 41
[35] Bardeen J and Stephen M 1964 *Phys. Rev.* **136** A1485
[36] Golubev D A and Dolgov O V 1993 unpublished
[37] Kuz'menko A B, Mena F P, Molegraaf H J A, van der Marel D, Gorshunov B, Dressel M, Mazin II, Kortus J, Dolgov O V, Muranaka T and Akimitsu J 2001 *Preprint* cond-mat/0107092
[38] Frederick N A *et al* 2001 *Physica* C **363** 1
[39] Brinkman A, Golubov A A, Rogalla H, Dolgov O V and Kortus J 2001 *Preprint* cond-mat/0111115